International Journal of Automotive and Mechanical Engineering
ISSN: 2229-8649 (Print); ISSN: 2180-1606 (Online)
Volume 16, Issue 4 pp. 7413-7429 Dec 2019

Performance Evaluation of CNT/MoS_2 Hybrid Nanofluid in Machining for Surface Roughness

Srinu Gugulothu[1*] and Vamsi Krishna Pasam[2]

[1]Mechanical Engineering Department, NIT Warangal, 506004, India
*Email: srinu72210@gmail.com
Phone No: +91 9989617091
[2]Mechanical Engineering Department, NIT Warangal, Telangana, 506004, India

ABSTRACT

Present work is motivated by the high thermal conductivity of MWCNT and low coefficient of friction due to MoS_2 nanoparticles which can significantly improve the heat transfer and lubrication performance of hybrid nanofluids than nanofluids. Hybrid nanofluids are prepared with CNT/MoS_2 nanoparticles of 1wt% in sesame oil, neem oil and mahua oil by varying hybrid ratio (i.e. 1: 1; 1:2 and 2:1) and surfactant. The hybrid nanofluid composition is evaluated based on stability analysis from sedimentation and zeta potential studies. The concentration of nanoparticles is varied by preparing CNT/MoS_2 hybrid nanofluid using obtained composition for stability and selected the optimal concentration for the lowest coefficient of friction obtained in friction test. The property of thermal conductivity is also evaluated for varying concentration of hybrid nanofluid at room temperature. The contact angle for CNT/MoS_2 hybrid nanofluids is evaluated with a contact angle meter to understand the lubrication effect. Experimental findings for stable hybrid nanofluid are found to be sesame oil, SDS with 15% content of nanoparticle weight and 1:2 hybrid ratio. From friction test, it is observed that 2 wt% concentration is optimal for least coefficient of friction (0.038). Minimum surface roughness (R_a) is observed with 2 wt% of hybrid nanofluid compared to dry machining and conventional cutting fluid. Optimum conditions for minimum surface roughness are evaluated in turning of AISI1040 steel with the use of 2wt% of CNT/MoS_2 hybrid nanofluid in RSM. R_a value is observed to decrease with an increase in cutting speed and increased with an increase in feed and depth of cut.

Keywords: CNT; MOS_2; solid lubricant; MQL; hybrid nanofluid; RSM

INTRODUCTION

Machining is one of the widely used manufacturing processes due to its ability to flexibly produce components to a high tolerance. In order to judge the quality of machining, surface finish and dimensional accuracy are the important aspects for producing various goods directly or indirectly. Power consumption during the machining is converted into heat energy at the cutting edge of the tool, which causes the temperature to rise in the cutting zone. Rise in temperature in contacting zone impact the dimensional accuracy and surface finish of the part being machined [1]. Main sources of heat generation during turning operation is the primary deformation zone and chip tool interface due to friction and very less amount of heat is generated due to rubbing action [2]. Friction on the rake face of the tool is reduced by applying the cutting fluids. Cutting fluid acts as a coolant at high cutting speed and lubricant at low speed, thus avoids the formation of built-up edge

(BUE) on cutting edge, which improves tool life and surface finish. Eighty percent of the cutting fluids used in metal cutting operations are mineral oil-based. But they possess various adverse effects, such as the risk of workers health in the industry, environmental pollution and high disposal cost [3]. Dry cutting, minimum quantity lubrication (MQL), solid lubricants, vegetable oil-based nanofluids are the various alternatives to the mineral oil-based cutting fluids [4]. MQL is the most advanced technology in the industry, which supplies minimum flow rate of the coolant on the contact zone with pressurized air thereby evaporates immediately. Amrita et al. [5] examined the performance of nano graphite added in water-miscible cutting fluid with different supply systems to cutting zone during machining. In system A, nanofluid was supplied through an MQL device with high pressure and 1mL/min flow rate. In system B, coolant was supplied with low pressure and 5 mL/min MQL flow rate. The cutting force (F_z) and cutting temperature (T) were found to be high for both the systems compared to flood machining. The lowest surface roughness (R_a) and tool flank wear (V_b) were obtained with both the systems compared to flood cooling and dry machining. Besides MQL, solid lubricants also play a key role in reducing machining performance in terms of F_z, T, R_a and V_b due to their structure and environment-friendly nature. Solid lubricants have layered structure, which has strong covalent bonding within the layer and weak Van der Waal's force of attraction between the layers, which enable to form strong lubricant film on contacting surfaces [4]. Boric acid, CaF_2, WS_2 and MoS_2 are some of the solid lubricants. Gunda et al. [6] studied the performance of MoS_2 in SAE oil in pin on disc test. 20 wt % of MoS_2 in SAE oil has provided superior performance in terms of reduction in the coefficient of friction (COF) and temperature in the sliding zone.

Vegetable oils (VOs) are highly recommended substitutes to the mineral oils for effective lubrication in machining due to their environmentally friendly nature and characteristics of less toxicity, high biodegradability and renewability [7]. VOs are primarily composed of triglyceride structure; whose molecular structure consists of three long-chain fatty acids connected to the hydroxyl group. VOs have high adsorption film formation capability on metallic surfaces and unsaturated long-chain fatty acids in VOs can react with metal surfaces forming a film like metallic soap. Both can improve antiwear and antifriction properties [8]. Ozcelik et al. [9] examined the performance of the various VOs with (8% and 12%) extreme pressure additives (EP) on F_z, R_a and V_b in turning of AISI304L. 8% EP included in canola oil performed better than other conditions in terms of reducing F_z, R_a and V_b.

Suspension of millimetre and micrometre-sized particle in base oils block the supply channels of cutting fluids due to quick settling. To restrict these challenges nano-sized particles are used. Nanofluids (NFs) are obtained by suspending nanoparticles with size less than 100 nm in base fluids like water, ethylene glycol etc. High heat carrying capacity of nanoparticles dispersed in the base fluid, less percentage by weight can enhance thermal properties of NFs due to their large surface to volume ratio and Brownian motion. Naik and Vinod [10] observed the enhancement in thermal conductivity (k) of NFs by adding Fe_2O_3, γAl_2O_3 and CuO nanoparticle in carboxymethyl cellulose base fluid in different concentrations. They inferred the increase in property k with an increase in concentration in the temperature range of (30-50°C). Similar findings were reported by researchers [11-13]. In addition to NFs, hybrid nanoparticle enriched fluids were outraging the machining performance in terms of reduction F_z, T and R_a due to improved properties than NFs [14, 15]. Suspending different nano-sized particles into BOs in the form of the composite mixture is termed as hybrid nanofluid (HNF). Sharma et al.[16] formulated the hybrid nanofluid by hybridizing, Al_2O_3(45 nm) and MoS_2(30 nm) nanoparticles at (90:10) volume proportion in (5% of vegetable oil +95% distilled water).They found that F_z was reduced by 7.35%, F_x was reduced by 18.08%, F_y was reduced by 5.73% and R_a was reduced by 2.38% by the application of (Al_2O_3 + MoS_2) HNFs compared to Al_2O_3 NFs.

Till date, very few investigations on HNFs were found in the open literature, especially by the application of VO based HNFs under MQL conditions in turning of AISI 1040 steel. In the current investigation, an attempt is made by the novel properties of HNFs especially in heat transfer and machining application. The solid lubricant of MoS_2 could improve the lubrication properties due to low COF and MWCNT improves heat transfer performance due to high property of *k*. Combination of both nanoparticles with certain hybrid ratio could enhance to a greater extent both the lubrication and cooling performance than NFs due to a physical synergistic effect. In the first phase of the present work, HNFs were prepared by taking three base oils, surfactants and CNT/MOS_2 nanoparticle at a concentration of 1 wt%. Thus, fluids were formulated using L_9 OA and CNT/MoS_2 HNF composition was evaluated by using sedimentation and zeta potential study. Taguchi method is used for selecting optimal factors for stability. In the second phase, evaluation of optimal concentration of CNT/MoS_2 (1:2) HNF by conducting friction test in varying concentration was done and R_a values were found with the use of 2 wt% of CNT/MoS_2 HNF in turning of AISI1040 steel under MQL mode. Response surface methodology is used to know the interaction 3D surface plot of control factors cutting speed (*V*), feed (*f*) and depth of cut (*d*).

MATERIALS AND METHODS

In the present work, nanomaterials of MWCNT (30 nm in outer diameter) and MoS_2 (30 nm) were purchased from Ishu international, New Delhi. Sesame oil (O_1), neem oil (O_2), mahua oil (O_3) and three surfactants were purchased from the local market. During experimentation, CNT/MoS_2 hybrid nanoparticles being coded as (x:y). Surfactants Tritonx100 and Tween80 were being named as Tx100 and Tw80 respectively. Saturated fatty acid (SFA) and unsaturated fatty acids (USFAs) composition of these three base oils are the demanding factors for their selection in the present work which enables to form strong lubricant film or layer and help in reducing friction on contacting surfaces [17].

Preparation of HNF

For improving stability of HNFs, Tx100, SDS and Tw80 surfactants were added in three different vegetable oils. Vegetable oil-based HNFs were prepared at a concentration of 1% by weight using the two-step method [3]. Three levels of base oil, surfactant, the content of surfactant and hybrid ratio (HR) were chosen as control factors for Taguchi's L_9 orthogonal array (OA) in preparation of HNFs. Piezo-U sonic homogenizer (frequency; 22.64 kHz) was used for ultrasonication of 3 hrs time after manual mixing. Chosen levels and control factors are depicted in Table 1.

Experimentation

For deciding the best composition for stable NFs, initially, stability analysis was performed by using sedimentation method and zeta potential study. Later, six samples of CNT/MoS_2 (1:2) HNFs were prepared using stable hybrid nanofluid compositions by varying concentration and COF was evaluated by using pin-on-disc apparatus.

To understand the dispersion behaviour of nanoparticles in the base oil, all the samples of prepared HNFs are poured in a beaker of 150mL each after ultrasonication and allowed to deposit for 156 hours at a particular location. Status of all the samples is recorded by taking photographs for every 12 hours. For measuring zeta potential value (ZPV), all the samples of HNF of each 5-10 mL was collected in measuring cell. Nanoparticle analyser (Horiba make, SZ 100 model) was used for measurement of ZPV. A solution with a range of zeta potential value 0 to ± 30 mV is said to be unstable and the particles coagulate, ± 30 to ± 40 mV fluid is moderately stable, while ± 40 to ± 60 mV fluid is more stable and more than ± 60 mV fluids is said to be in excellent stability.

In the second phase of present work, after deciding HNF composition from stability analysis, CNT/MoS$_2$ (1:2) HNF was prepared by varying mass concentration of 0.5%, 1%,1.5%, 2%,2.5% and 3 wt%. Thus, fluids were subjected to measurement of thermal conductivity using thermal conductivity analyser (make: Hot disk and model: TPS500) at room temperature. The tribological property of COF and contact angle were measured using Pin-on disc Tribometer (make: Magnum Engineers) and contact angle meter (Make: Holmarc, model: HO-IAD-CAM-01) respectively. Dimensions of pin and disc used were 28mm length, 10mm diameter and 165mm pitch circle diameter, 8mm thickness respectively. The material used for pin and disc were AISI 1040 steel and EN31 steel respectively. Load, speed of disc and measuring time used during friction test were 200 N, 200 rpm and 5 min respectively. Wear debris on the disc were removed by using 1000no carbon emery paper after each experiment. Average of triplicate values were considered in the analysis.

Table 1. Chosen levels and control factors

Control factors	Level		
	1	2	3
Base oil	O$_1$	O$_2$	O$_3$
Surfactant	Tx100	SDS	Tw80
Content of surfactant	5%	10%	15%
HR	1:1	1:2	2:1

The ability of a fluid to spread uniformly over another liquid or solid, forming a thin or continuous film, the fluid surface with high surface tension ensures a little or no wetting ability; those with low surface tension leads to high wetting ability. Wettability of fluids is understood by measuring the contact angle between a droplet of liquid and solid hot surface (cutting tool). On the other hand, this macroscopic contact angle is viewed as an interaction of intermolecular forces acting on the contact line. Systems free energy depends on intermolecular forces acting on the contact line, which gets the phenomenon of higher surface tension. The net surface tension of liquid droplet depends on Van der Waals forces [24]. Interaction length of these forces was equivalent to nanoparticle size in nanometer. Hence, the addition of nanoparticles has an effect on the total free energy of solid, liquid and air interface. For testing, this hypothesis wettability characteristics of base oil and HNF samples in varying particle concentration (0.5 to 3 wt %) of CNT/MoS$_2$ was measured with contact angle meter (Make: Holmarc, model: HO-IAD-CAM-01). All measurements were carried out at 27°C temperature and droplet volume of 10 µl was used in experiments which were ensured with a micro metering syringe. This contact angle is determined with young’s Eq. (1). Schematic showing liquid droplet on a solid surface is presented with Figure 1.

$$\cos\theta = \frac{\text{Net adhesion force}}{\text{Surface tention force}} = \left(\frac{\sigma_{sv}\text{-}\sigma_{sl}}{\sigma_{lv}}\right) \quad (1)$$

where θ is the angle between the droplet and horizontal solid surface, σ_{sv}, σ_{sl}, and σ_{lv} are the solid-vapour, solid-liquid and liquid vapour interfacial tensions.

Machining of AISI1040 steel was performed on a lathe (Magnum make, 10 hp power capacity) with carbide insert (CNMG120408TTS; widia make) by varying cutting conditions [17]. The experimental setup for turning under MQL is shown in Figure 2. The carbide insert was clamped with screw-on (PCLNR2525M120; widia make) tool holder during machining. The 2 wt% of CNT/ MoS_2 (1:2) HNF was supplied to cutting zone with MQL system during machining with variable cutting conditions presented in Table 2. The compressor air pressure was always maintained at 4bar for supplying the fluid to machining zone at a flow rate of 10 mL/min. The value of R_a was measured after each turning operation by using the Taylor Hobson surface roughness tester (model: Surtronic S128). The average value of three experimental trials was considered in the analysis.

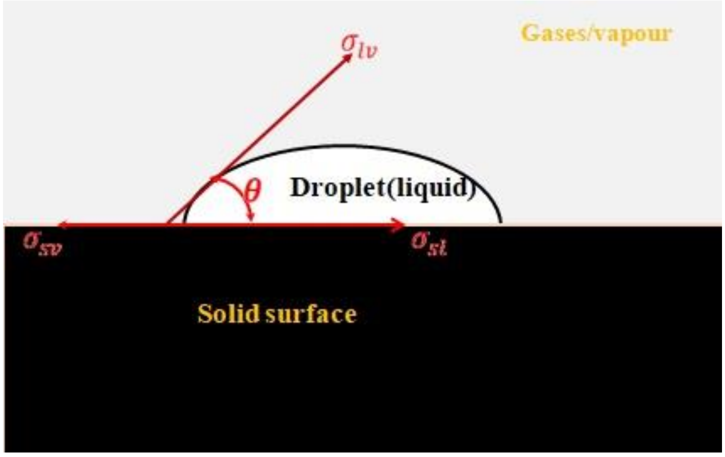

Figure 1. Schematic representation of droplet of liquid on a solid surface.

Taguchi Robust Design

Taguchi's L_9 OA is mainly adopted for the setting of optimal control parameters. In this study, ZPV is the response parameter for optimisation. Higher ZPV is the indication of highly stable HNFs. Therefore, the criterion of larger the better type is chosen for this study.

$$\frac{S}{N}\, ratio\ (\eta) = -10 \log\left[\ \frac{1}{n}\sum_{i=1}^{n}\frac{1}{y^2}\ \right] \quad (2)$$

where, terms "y" and "n" are response parameter and number of replications. Analysis of Variance (ANOVA) is a hypothesis-testing technique used to find the order of contributing factors for response parameters by testing the equality of two or more treatment means. It gives effects of each factor on machining output parameters.

Response Surface Methodology

RSM is one of the best statistic techniques used for creating model build up the relationship between experimental input and output response parameters. Each and every response (y) is influenced by different input factors (x_i, $x_{j,..}$). The established correlation between independent input factors and response variable is presented with the following polynomial Eq. (3).

$$y=f(x_1, x_2, x_3 \ldots\ldots x_k) \tag{3}$$

The first-order model is not used for optimisation due to lack of fit. The second-order model improves optimisation for the response variable due to more interaction effects of the several independent input factors. A general form of the second-order model is represented as

$$y = a_0 + \sum_{i=1}^{n} a_i x_i + \sum_{i=1}^{n} a_{ii} x_i^2 + \sum_{i=1}^{n} \sum_{j=1}^{n} a_{ij} x_i x_j : i < j \tag{4}$$

where, term a_0 is constant, a_i, a_{ii}, a_{ij} are the coefficients for the quadratic model and x_i, x_j are the input factors

Cutting parameters were optimised with Box-Behnken design in RSM tool to get desired response value. Levels chosen in Box-Behnken design are low, medium and high which are coded as -1, 1 and 1. A total 15 experimental runs were considered in this design with three center points. The independent input factors with their values and levels chosen in the present work are presented in Table 2 and response variables noted during machining are presented in Table 6. For experimental design and building of the model, design expert software was used. The regression analysis of experimental data is also carried out by using the same. The quality of the fit for the second-order model is checked with the value of R^2 and adjusted R^2. The point optimisation was used for multiple response parameters and values of optimal setting parameters were found.

Figure 2. Experimental setup for MQL turning.

Table 2. Factors and levels chosen.

Factors		Levels		
		-1	0	+1
V	(m/min)	60	80	100
F	(mm/rev)	0.131	0.161	0.191
d	(mm)	0.5	0.75	1

RESULTS AND DISCUSSION

Stability Analysis

ZPV of CNT/MoS_2 HNF is presented in Table 3. Figure 3 presents sedimentation test results after 156 hours of sedimentation time of CNT/ MoS_2 HNF. From the sedimentation test, no sedimentation is observed in sample 2 and sample 3. Air bubbles are observed in sample 8 and sample 9 at the bottom of the beaker thus gave less sedimentation compared to sample 2 and sample 3. The sample with no sedimentation gives highest ZPV which is in the range of ±50 mv and above. An increased ZPV shows the increase of repulsion forces between the charged nanoparticles due to the formation of double-layer [18]. It is observed that inclusion of SDS and Tw80 surfactants in O_1 along with CNT/ MoS_2 nanoparticles gave no sedimentation whereas other samples have given less, moderate and highest. A surfactant forms a coat on the nanoparticles and prevents aggregation by causing repulsive forces between nanoparticles [19]. Dispersion of CNT/ MoS_2 nanoparticle along with SDS in O_1 has given highest ZPV among all samples of HNFs. This shows excellent stability [18]. This is possible with the dispersion of SDS surfactant in O_1 due to hydrophobic characteristics of SDS and its good compatibility with CNT nanoparticle [20].

Table 3. ZPVs of CNT/MoS_2 (1:2) HNF

Experimental Run	Factors				ZPV (mV)
	Base oil	Surfactant	Content of surfactant	Hybrid mixing ratio	
1	O_1	Tx100	5%	1:1	-77.2
2	O_1	SDS	10%	1:2	96.1
3	O_1	Tw80	15%	2:1	105.4
4	O_2	Tx100	10%	2:1	22.5
5	O_2	SDS	15%	1:1	-42.7
6	O_2	Tw 80	5%	1:2	-37.7
7	O_3	Tx100	15%	1:2	-106.8
8	O_3	SDS	5%	2:1	-67.6
9	O_3	Tw80	10%	1:1	-54.4

Figure 3. Sedimentation test results after 156 hours.

Table 4. ANOM of S/N ratios for ZPV of CNT/ MoS$_2$(1:2) HNF.

Level	Base oil	Surfactant	Content of surfactant	Hybrid mixing ratio
1	39.34	35.12	35.29	35.02
2	30.39	36.29	33.80	37.25
3	37.29	35.62	37.94	34.76
Delta	8.95	1.16	4.13	2.49
Priority	1	4	2	3
Optimum	A$_1$	B$_2$	C$_3$	D$_2$

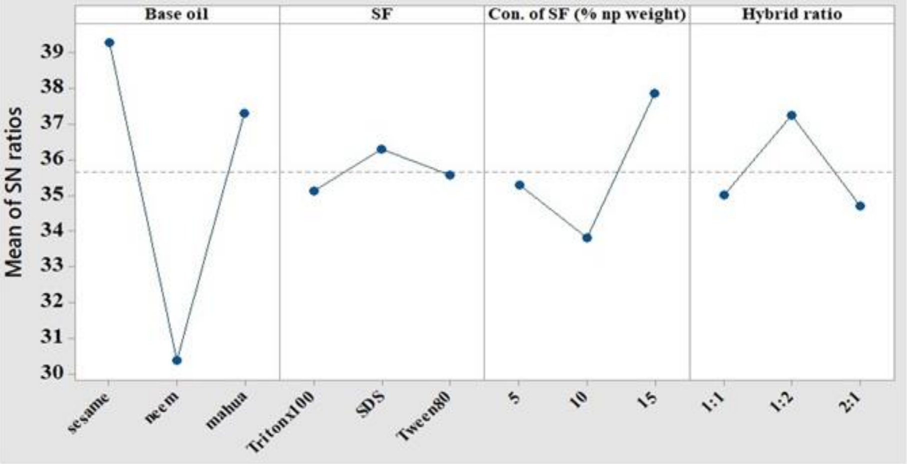

Figure 4. Main effect plot for S/N ratios for ZPV.

Analysis of mean (ANOM) is performed by using Taguchi's S/N ratio technique for finding HNF composition and their influence on ZPV by considering larger-the-better criterion. Table 4 presents the ANOM of S/N ratio of ZPV for CNT/MoS$_2$ HNFs. From the results, it is observed that the order of influencing factors on ZPV could be base oil, the content of surfactant, hybrid mixing ratio and surfactant type. From Taguchi analysis, optimal setting parameters are found to be O$_1$, SDS with 15% by weight of nanoparticle and hybrid mixing ratio (1:2) for stability analysis of CNT/MoS$_2$ HNF which are peak values shown Figure 4. ANOVA is used to study the individual effect of each control factors on ZPV. From the results, the order of contributing factors could be base oil contributing (77%) followed by surfactant concentration (15.3%), HR (6.5%) and surfactant type (1.2%) as shown in Table 5. From the confirmation test results, no sedimentation is observed and the highest ZPV of 107.5 mV obtained represents excellent stability as shown in Figure 5.

Table 5. ANOVA of ZPV of (S/N data) of CNT/ MoS_2 (1:2) HNF

Source	DOF	SS	MS	% contribution
Base oil	2	131.969	65.9847	77
Surfactant	2	2.049	1.0245	1.2
Content of surfactant	2	26.285	13.1423	15.3
Hybrid mixing ratio	2	11.249	5.6246	6.5
Residual error	0			
Total	8	171.552		100

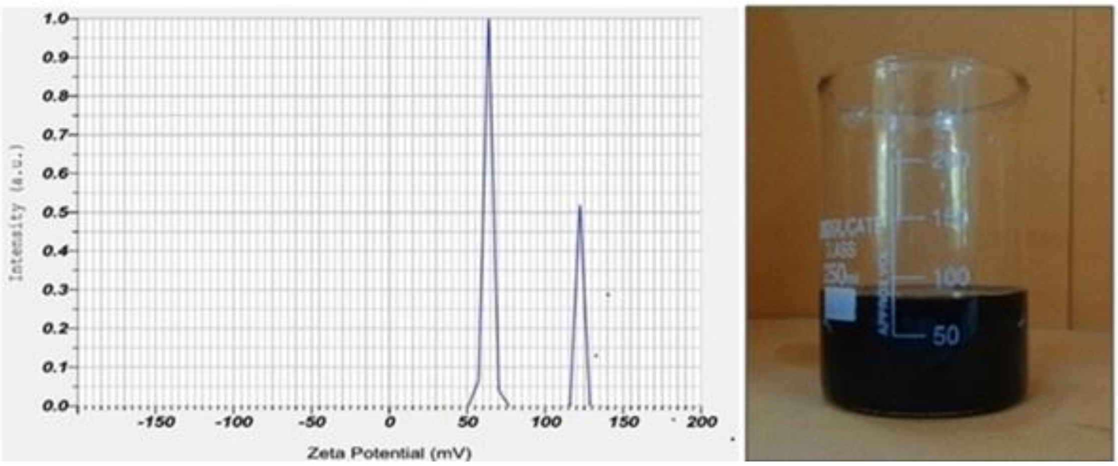

(a) (b)

Figure 5. (a)ZPV report of CNT/ MoS_2 (1:2) HNF (ZPV with peak 1 and peak 2 at 122.0 mV, 63.4 mV and the average is 107.5 mV). (b) Sedimentation results of confirmation sample for 156 hours

Results of thermal conductivity of CNT/MoS_2 HNF by varying concentration are depicted in Table 6. From the results, it is observed that the property of the thermal conductivity is slightly increased with increase in the concentration of CNT/MoS_2 nanoparticle in the base oil. Thermal conductivity of HNFs is found to be improved compared to the thermal conductivity of sesame oil (0.1764 W/m.K) at room temperature. This may be due to shape, size and Brownian motion of nanoparticle.

Table 6. Thermal conductivity of the CNT/MoS_2 HNF.

Concentration of nanoparticle (wt%)	0	0.5	1	1.5	2	2.5	3
Thermal conductivity at Room temperature (W/m.K)	0.1864	0.2174	0.2193	0.2228	0.2238	0.2257	0.2263

Coefficient of Friction and Contact Angle

Results of COF under different lubrication environment are shown in Figure 6. COF decreased with increase in particle concentration up to 2 wt% and then slightly increased.

This may be due to aggregation of nanoparticles at higher concentration [21]. The least COF is found to be 0.038 at concentration 2 wt% of CNT/ MoS$_2$ (1:2) HNF among other samples. COF is found to reduce by 93.77% and 83% with the use of 2 wt% of CNT/ MoS$_2$ (1:2) HNF than that of the dry condition and base oil respectively. This affirmative performance of HNFs is due to structure, size and shape of nanomaterials and long-chain USFAs profiles in O$_1$ [22]. When CNT and MoS$_2$ nanomaterials are combined in the proportion of 1:2 in O$_1$, it tremendously reduces COF on the contact surface (workpiece and cutting tool) due to their physical synergic effect and ball-bearing effect as shown in Figure 7 and reported by Zhang et al. [23]. After analysing COF results, we can conclude that before 2 wt% of nanoparticle concentration, the coefficient of friction is inversely proportional to nanoparticle concentration. This reflects that the lubrication performance of hybrid nano cutting fluids is improved gradually. After the 2 wt%, the coefficient of friction is proportional to nanoparticle concentration, which reflects that lubrication performance of the hybrid nano cutting fluid decreases gradually. The reason could be the agglomeration of nanoparticles at higher concentration.

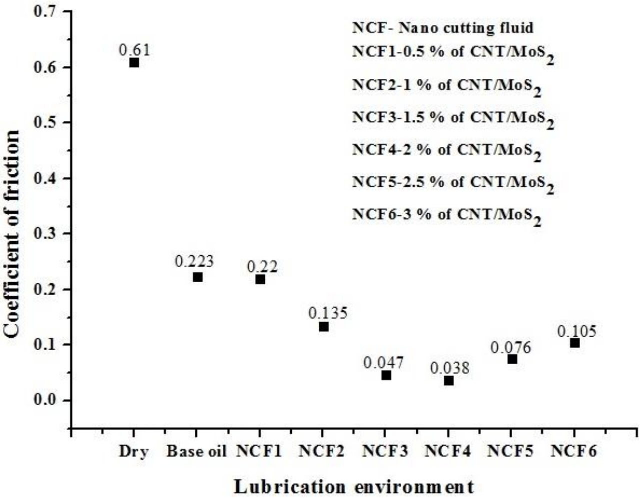

Figure 6. Coefficient of friction versus lubrication environment.

The spreadability of hybrid nanoparticles enriched cutting fluid is influenced by the percentage of nanoparticles. The contact angle between fluid droplet and the solid surface of the base fluid and HNFs are depicted in Figure 8. As the concentration of hybrid nanoparticle (CNT/MoS$_2$) increases from 0.5to 2.5 wt%, the contact angle is increased first, then slightly reduced for a particle concentration of 3 wt%. Among the all prepared samples of HNFs, the lowest contact angle is found to be (8.07°) at 0.5 wt% concentration for CNT/MoS$_2$ (1:2) HNF. Thus, gave maximum wetting area per unit volume of fluid [24]. Based on the literature, the contact angle is less for more wettability. However, wettability is not only the one criterion for improvement in lubrication performance; it also depends on several factors. Of such are bonding between the nanoparticles, particle-fluid interactions and low range electrostatic force of interactions between the nanoparticles that depend on nanoparticle concentration and size [25]. The contact angle of the base oil is recorded as (34.98°) which is much higher compared to hybrid nano cutting fluid. The experimental data clearly suggested that the wettability of hybrid nanofluids is affected by the addition of nanoparticle in the base oil. This can be justified by the findings of Wasan et al. [26]. The wetting area per unit volume of fluid is increased in the case of hybrid nano cutting fluid compared to the base oil. It is the fact that higher contact area of coolant with hot solid surface, higher would be the heat transfer from the hot surface [27]. Hence it enhances the lubrication effect and heat extraction properties compared to base oil.

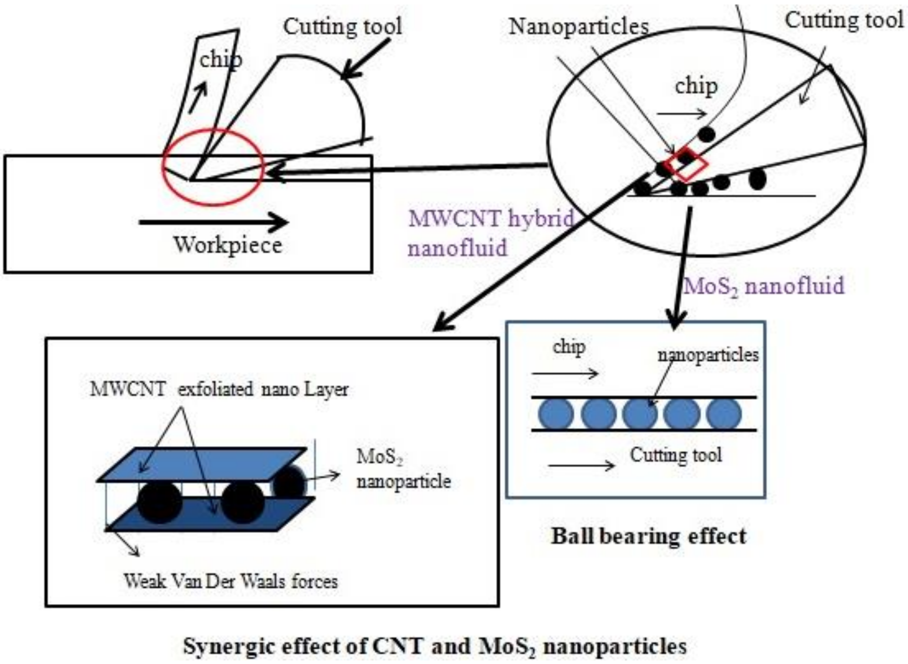

Figure 7. Synergic effect and ball-bearing effect of CNT/MoS2 nanoparticles in during sliding surfaces [23].

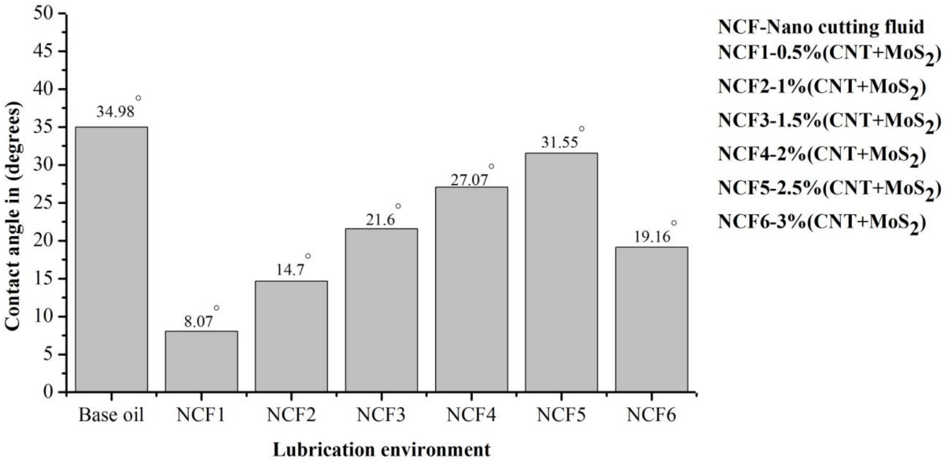

Figure 8. Contact angle with respect to nanoparticles concentration.

Surface Roughness (R_a) Under Different Lubrication Environment

Surface quality mainly depends on the surface finish of the machined product. Good surface finish is achieved by minimising heat at the chip-tool interface by the application of cutting fluid. Surface roughness (R_a) is measured by using surface roughness tester under dry machining, CCF and HNF at constant cutting conditions (V = 80 m/min, f = 0.161 mm/rev and d = 0.5 mm) during turning of AISI 1040 steel. Results of R_a in varying lubrication conditions are shown in Figure 9. The highest value of R_a is obtained under dry machining is 2.8 µm, followed by CCF at 2.45 µm and 2 wt% of HNF at 2.0 µm. R_a value is found to reduce by 29% and 18.5% by the application of 2 wt% of HNF compared to dry machining and CCF respectively. Consistent film formation on contacting surfaces, stable form of nanofluid and proper bonding between the nanoparticles are the reason for this improvement.

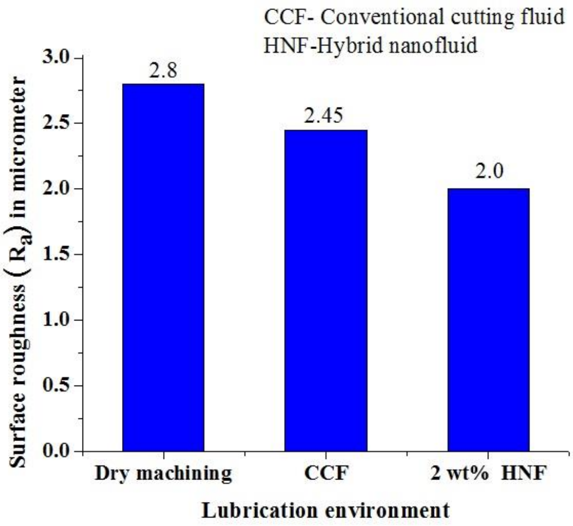

Figure 9. Variation of the surface roughness in different lubrication environment at *V*= 80 m/min, *f*= 0.161 mm/rev and *d*= 0.5 mm.

Surface Roughness (R_a) with Varying Cutting Conditions

Turning of AISI 1040 steel is also carried out by varying cutting conditions as per experimental design and responses in Table 7. The variance of surface roughness value during machining are analysed with an objective of influence of cutting parameters on R_a.

The influence of cutting parameters *V*, *f* and *d* by using 2 wt% of CNT/MoS_2 (1:2) HNF on R_a is illustrated in Figure 10(a) to 10(c). R_a value is observed to decrease and then increase with the cutting parameter V due to the vanishing of BUE on tooltip at high speed. R_a value increased with increase in *f* and *d* due to axial movement of tool and rigidity effect of the machine. The lowest R_a value of 1.33 µm is achieved with interaction of *f* = 0.131 mm/rev and *d*=0.5mm at *V*=80m/min. The increase in *V* causes easier plastic deformation and chip flow during machining which reduces the built-up edge formation on the tool and improves the surface quality of the machined part [28]. The results of ANOVA are depicted in Table 8. P-value of the model 0.0009 which is less than 0.05 indicates that the model is significant [29]. The model terms *V* and *f* are significant where *d* is not significant on R_a value. The non-significant terms are not counted in the building of models. The regression model R_a with the values of R^2 and adjusted R^2 are equal to 0.9806 and 0.9455. R^2 predicted value is 0.7340 and adequate precision value is 18.188. The R^2 predicted value is in good agreement with the value of adjusted R^2. From the R^2 value and adequate precision value, it is understood that the developed model is desirable for prediction of R_a value. The mathematical model or regression model developed by using response surface methodology gives a relationship between the machining response variable and input cutting condition. Hence, the regression model developed for R_a is as follows in Eq. (5).

$$\text{Surface roughness } (R_a) = -2.98389-0.16906\times V+123.16944\times f+4.49167\times d + 0.25000\times v\times f +0.021500\times v\times d-13.3333\times f\times d+0.0006531\times V^2 -390.1019\times f^2-2.78000\times d^2 \quad (5)$$

Table 7. Machining input cutting conditions and surface roughness value (R_a)

Run order	Input machining parameters			R_a (µm)
	V (m/min)	*f* (mm/rev)	*d* (mm)	
1	60	0.131	0.75	2.1
2	80	0.131	1	1.4
3	60	0.191	0.75	2.3
4	80	0.191	1	1.6
5	80	0.161	0.75	2.07
6	100	0.161	1	2.17
7	100	0.131	0.75	1.4
8	80	0.191	0.5	1.93
9	100	0.191	0.75	2.2
10	80	0.131	0.5	1.33
11	80	0.161	0.75	2.15
12	80	0.161	0.75	2.05
13	60	0.161	0.5	2.4
14	100	0.161	0.5	1.93
15	60	0.161	1	2.21

Table 8. ANOVA table for R_a.

Source	SS	DF	MS	F-value	P-value	Remarks
Model	1.67	9	0.19	28.01	0.0009	Significant
V	0.21	1	0.21	32.38	0.0023	
F	0.40	1	0.40	61.13	0.0005	
D	5.513E-003	1	5.513E-003	0.83	0.4035	
*V*f*	0.090	1	0.090	13.58	0.0142	
*V*d*	0.046	1	0.046	6.98	0.0459	
*f*d*	0.040	1	0.040	6.04	0.0574	
V^2	0.25	1	0.25	38.04	0.0016	
f^2	0. 46	1	0.46	68.76	0.0004	
d^2	0.11	1	0.11	16.83	0.0093	
Residual	0.033	5	6.625E-003			
Lack of fit	0.028	3	9.175E-003	3.28	0.2425	not significan
Pure error	5.600E-003	2	2.800E-003			
Cor. total	1.70	14				

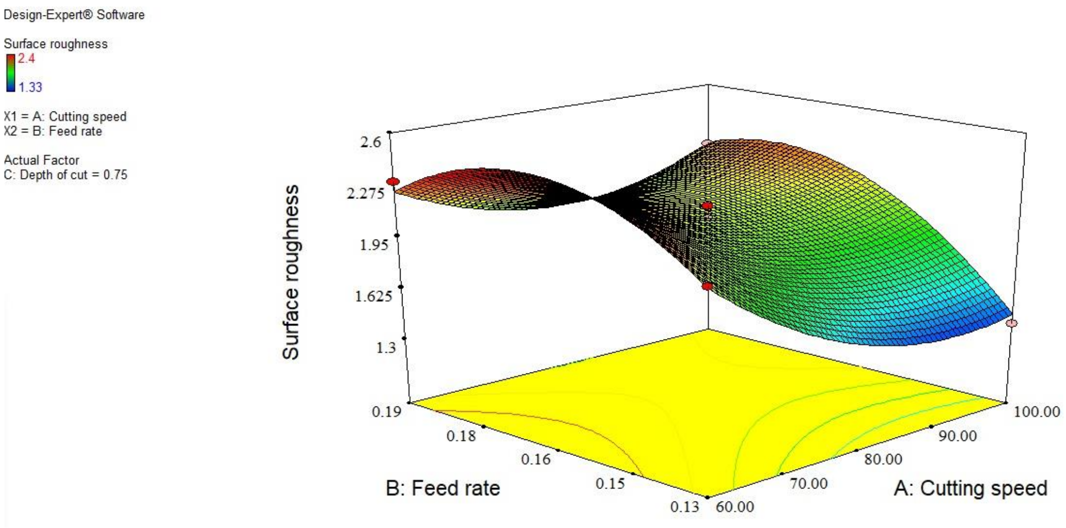

(a) feed rate and cutting speed

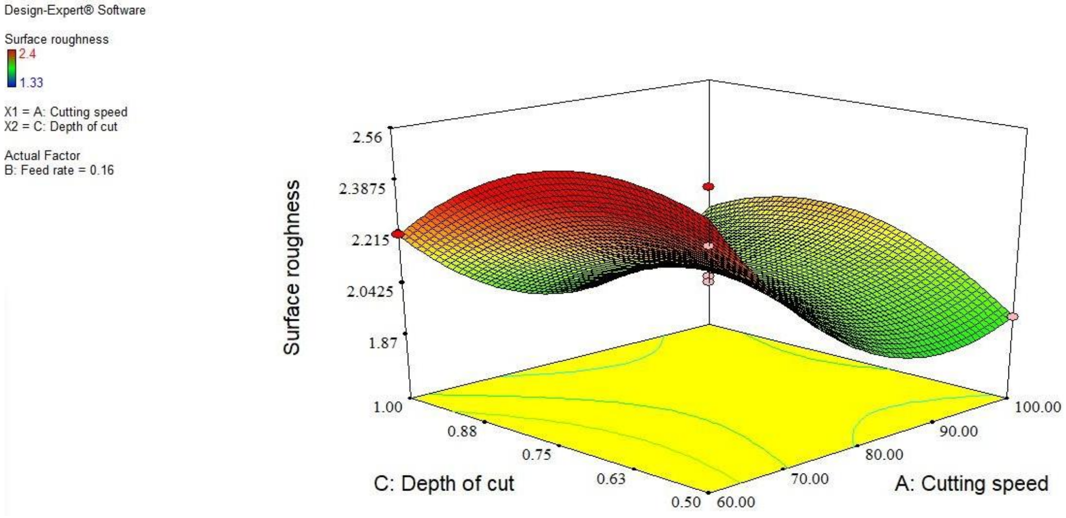

(b) depth of cut and cutting speed

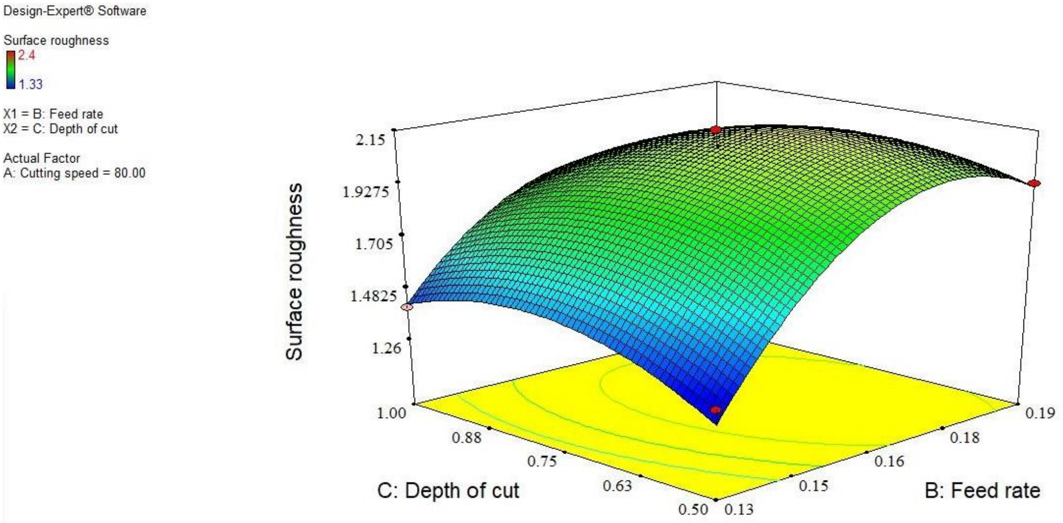

(c) depth of cut and feed rate

Figure 10. Response surface plot R$_a$ responding to cutting parameters.

CONCLUSION

Following conclusions are drawn from stability analysis, friction test by varying concentration of CNT/MoS2 (1:2) in sesame oil and turning of AISI 1040 steel under MQL condition.

i. The stability analysis from sedimentation and zeta potential test, optimal setting parameters for stable nanofluid are found to be O1, SDS with 15% concentration and hybrid mixing ratio of 1:2.
ii. Thermal conductivity of the HNF increased with nanoparticle concentration.
iii. Lowest coefficient of friction (0.038) is achieved with 2 wt% of CNT/MoS2 (1:2) HNF among the other samples.
iv. The concentration of 0.5 wt. % of CNT/MoS2 HNF showed the lowest contact angle of 8.07° which gives better wettability among the other conditions.
v. R_a is reduced by 29% and 18.5% with 2 wt% of HNF under MQL mode compared to dry machining and conventional cutting fluid respectively.
vi. Cutting speed and feed rate is significant on Ra value whereas depth of cut has no significance. With an increase in cutting speed, R_a value is found to decrease and increase with an increase in feed and depth of cut.
vii. Lowest R_a value of 1.33 µm is observed at 0.131 mm/rev feed, 0.5 mm depth of cut and cutting speed of 80m/min.

REFERENCES

[1] Bhattacharyya A. Metal cutting: theory and practice. Jamini Kanta Sen of Central Book Publishers; 1984.

[2] Akhil CS, Ananthavishnu MH, Akhil CK, Afeez PM, Akhilesh R, Rahul R. Measurement of cutting temperature during machining. IOSR Journal of Mechanical and Civil Engineering (IOSR-JMCE). 2016;13(2):108-122.

[3] Amrita M, Srikant RR, Raju AS. Performance evaluation and economic analysis of minimum quantity lubrication with pressurized/non-pressurized air and nanofluid mixture. International Journal of Mechanical, Aerospace, Industrial, Mechatronic and Manufacturing Engineering. 2015; 9(6):946-951.

[4] Krishna PV, Rao DN. Performance evaluation of solid lubricants in terms of machining parameters in turning. International Journal of Machine Tools and Manufacture. 2008; 48(10):1131-1137.

[5] Amrita M, Srikant RR, Sitaramaraju AV, Prasad MM, Krishna PV. Preparation and characterization of properties of nanographite-based cutting fluid for machining operations. Proceedings of the Institution of Mechanical Engineers, Part J: Journal of Engineering Tribology. 2014; 228(3): 243-252.

[6] Gunda RK, Narala SK. Evaluation of friction and wear characteristics of electrostatic solid lubricant at different sliding conditions. Surface and Coatings Technology. 2017; 332:341-350.

[7] Lawal SA, Choudhury IA, Nukman Y. Application of vegetable oil-based metalworking fluids in machining ferrous metals—a review. International Journal of Machine Tools and Manufacture. 2012 Jan 1; 52(1):1-2.

[8] Wang Y, Li C, Zhang Y, Yang M, Li B, Jia D, Hou Y, Mao C. Experimental evaluation of the lubrication properties of the wheel/workpiece interface in minimum quantity lubrication (MQL) grinding using different types of vegetable oils. Journal of Cleaner Production. 2016; 127:487-499.

[9] Ozcelik B, Kuram E, Cetin MH, Demirbas E. Experimental investigations of vegetable based cutting fluids with extreme pressure during turning of AISI 304L. Tribology International. 201; 44(12):1864-871.

[10] Naik BA, Vinod AV. Rheological behaviour and effective thermal conductivity of non-Newtonian nanofluids. Journal of Testing and Evaluation. 2017; 46(2).

[11] Wei B, Zou C, Li X. Experimental investigation on stability and thermal conductivity of diathermic oil based TiO2 nanofluids. International Journal of Heat and Mass Transfer. 2017; 104:537-543.

[12] Turgut A, Tavman I, Tavman S. Measurement of thermal conductivity of edible oils using transient hot wire method. International journal of food properties. 2009; 12(4):741-747.

[13] Su Y, Gong L, Li B, Chen D. An experimental investigation on thermal properties of molybdenum disulfide nanofluids. InProceedings of the 2015 International Conference on Materials, Environmental and Biological Engineering, edited by G. Zhang and M. Lee (AER-Advances in Engineering Research, Guilin, China, 2015 (pp. 881-885).

[14] Nabil MF, Azmi WH, Hamid KA, Zawawi NN, Priyandoko G, Mamat R. Thermo-physical properties of hybrid nanofluids and hybrid nanolubricants: a comprehensive review on performance. International Communications in Heat and Mass Transfer. 2017; 83:30-39.

[15] Zareie A, Akbari M. Hybrid nanoparticles effects on rheological behaviour of water-EG coolant under different temperatures: An experimental study. Journal of Molecular Liquids. 2017; 230:408-414.

[16] Sharma AK, Singh RK, Dixit AR, Tiwari AK. Novel uses of alumina-MoS 2 hybrid nanoparticle enriched cutting fluid in hard turning of AISI 304 steel. Journal of Manufacturing Processes. 2017; 30:467-482.

[17] Pasam VK, Gugulothu S. Testing and Performance Evaluation of Vegetable-Oil–Based Hybrid Nano Cutting Fluids. Journal of Testing and Evaluation. 2018; 48(5).

[18] Venkataraman M. The effect of colloidal stability on the heat transfer characteristics of nanosilica dispersed fluids. M.Sc. Thesis, University of Central Florida Orlando, Florida.1-93.

[19] Niyaghi F, Haapala KR, Harper SL, Weismiller MC. Stability and biological responses of zinc oxide metalworking Nanofluids (ZnO MWnF™) using dynamic light scattering and zebrafish assays. Tribology Transactions. 2014; 57(4):730-739.

[20] Vaisman L, Wagner HD, Marom G. The role of surfactants in dispersion of carbon nanotubes. Advances in colloid and interface science. 2006; 128:37-46.

[21] Padmini R, Krishna PV, Rao GK. Effectiveness of vegetable oil based nanofluids as potential cutting fluids in turning AISI 1040 steel. Tribology International. 2016; 94:490-501.

[22] Zhang Y, Li C, Jia D, Zhang D, Zhang X. Experimental evaluation of MoS2 nanoparticles in jet MQL grinding with different types of vegetable oil as base oil. Journal of Cleaner Production. 2015; 87:930-940.

[23] Zhang Y, Li C, Jia D, Zhang D, Zhang X. Experimental evaluation of the lubrication performance of MoS2/CNT nanofluid for minimal quantity lubrication in Ni-based alloy grinding. International Journal of Machine Tools and Manufacture. 2015; 99:19-33.

[24] Khandekar S, Sankar MR, Agnihotri V, Ramkumar J. Nano-cutting fluid for enhancement of metal cutting performance. Materials and Manufacturing Processes. 2012 Sep 1; 27(9):963-7.

[25] Cieśliński JT, Krygier KA. Sessile droplet contact angle of water–Al2O3, water–TiO2 and water–Cu nanofluids. Experimental Thermal and Fluid Science. 2014; 59:258-263.

[26] Wasan D, Nikolov A, Kondiparty K. The wetting and spreading of nanofluids on solids: Role of the structural disjoining pressure. Current Opinion in Colloid & Interface Science. 201; 16(4):344-349.

[27] Singh RK, Sharma AK, Dixit AR, Tiwari AK, Pramanik A, Mandal A. Performance evaluation of alumina-graphene hybrid nano-cutting fluid in hard turning. Journal of cleaner production. 2017; 162:830-45.

[28] Sarıkaya M, Güllü A. Multi-response optimisation of minimum quantity lubrication parameters using Taguchi-based grey relational analysis in turning of difficult-to-cut alloy Haynes 25. Journal of Cleaner Production. 2015; 91:347-357.

[29] Gopalakannan S, Senthilvelan T. Optimisation of machining parameters for EDM operations based on central composite design and desirability approach. Journal of Mechanical Science and Technology. 2014; 28(3):1045-53.